

## The Wavelength Dependence of Pulse Dispersion in Multimode Fibre Optical Waveguides

HARISH R. D. SUNAK

*Instituto de Física, Universidade Estadual de Campinas, 13100 Campinas, SP, Brasil*

Recebido em 19 de Dezembro de 1979

Pulse dispersion measurements were carried out on solid- and liquid-core multimode optical fibres having step-index difference between core and cladding at three wavelengths, namely 694, 782 and 871 nm. It was found that provided launching was done at the same numerical aperture, there was negligible difference in pulse dispersion at the three wavelengths. Measurement of the output angle from the fibre indicated that the established mode distribution was also nearly equal in each case.

Medidas de dispersão de pulso foram concluídas em fibras Óticas multimodo de núcleo sólido e líquido com perfil de índice degrau em três comprimentos de onda, 694, 782 e 871 nm. Foi verificado que se o lançamento foi feito na mesma abertura numérica, houve uma diferença desprezível na dispersão de pulso nos três comprimentos de onda. Medidas do ângulo de saída no final da fibra indicavam que a distribuição de modos estabelecida também era aproximadamente igual em cada caso.

### 1. INTRODUCTION

There is a great interest in optical fibres at the moment, in Brazil, aimed at the eventual development of fibre optical communication systems for diverse applications. Fibres are now being pulled routinely at the "Padre Roberto Landell de Moura" Research and Development Centre of TELEBRAS in Campinas and various measurements done there, as well as in our laboratories in UNICAMP, to assess the quality of these fibres. We have already reported results of measurements made to de-

termine normalised mode conversion coefficients in these fibres. Further, we have developed a Nanosecond Test Facility<sup>2</sup> to carry out a detailed and systematic study<sup>3</sup> of modal dispersion and material dispersion<sup>4</sup> in TELEBRAS fibres.

Dispersion in multimode fibres is dominated completely by the differences in the group velocities of the various modes propagating in the fibre<sup>3,5</sup>. Various terms have been used to describe this type of dispersion and include: modal dispersion, multi-mode or multi-path dispersion, waveguide dispersion and monochromatic dispersion. This dispersion can be assessed from the broadening<sup>3</sup> that occurs in a short (e. g. sub-nanosecond) pulse after propagation in the fibre. Short pulses are readily obtained from mode-locked<sup>6</sup> lasers and pulse dispersion measurements have been carried out with different lasers operating at different wavelengths. Some of these lasers include, for example, He-Ne<sup>7</sup> (output wavelength 633 nm); Nd: YAG<sup>8</sup> (1.06  $\mu\text{m}$ ), krypton-ion<sup>9</sup> (647, 568 nm), dye<sup>10</sup> (588 nm), frequency doubled Nd: Glass<sup>11</sup> (530 nm), Stokes wavelength (871 nm) from acetone<sup>12</sup> with stimulated Raman scattering using a mode-locked ruby laser<sup>13</sup> as the pump. In addition, short pulses have been obtained, by suitably modulating GaAs lasers<sup>3</sup> operating in the 800-900 nm region. Since modal dispersion is dependent on many parameters and launching conditions, (see, for example, references 3, 5, 14, 15), we carried out<sup>5</sup> a systematic study at 694, 782 and 871 nm to determine whether there was any significant dependence of modal dispersion on the wavelength of the probe pulse and this paper outlines the results obtained. This was essential to explain any discrepancies in the measurements under different conditions using various laser sources. The results obtained are compared and discussed with other similar measurements<sup>8,9</sup>.

## 2. EXPERIMENTAL SET-UP

The experimental set-up used for the measurements is shown in figure 1. The source of the light pulses was a mode-locked ruby laser<sup>13</sup>. Since the repetition rate of the laser was  $\sim 1$  Hz, a sampling oscilloscope, normally used to display the pulses in dispersion measurements,

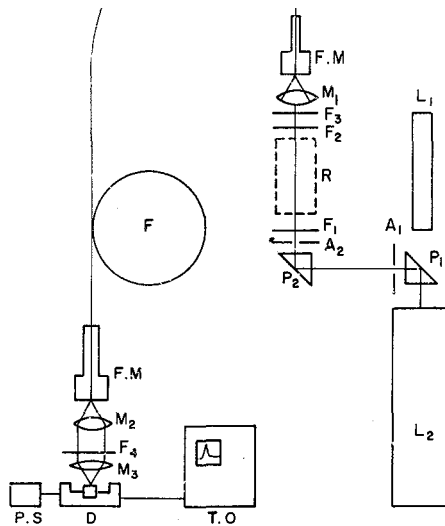


Fig.1 - Experimental set-up used to investigate modal dispersion as a function of wavelength. L<sub>1</sub> - He-Ne alignment laser; L<sub>2</sub> - pulsed mode-locked ruby laser; P<sub>1</sub>, P<sub>2</sub> - prisms of BK7 glass; A<sub>1</sub>, A<sub>2</sub> - apertures, removed after alignment of ruby beam; F<sub>1</sub>, F<sub>3</sub> - neutral density filters; F<sub>2</sub> - cut-off filter at 694 nm, when needed; F<sub>4</sub> - narrow band-pass filters; R-Raman cell; M<sub>1</sub> - coupling objective or lens; F.M. - fibre mount with index matching liquid; F - fibre under test; M<sub>2</sub> - microscope objective (x45); M<sub>3</sub> - microscope objective (x10); D - Tropel 330 photodetector; P.S. - power supply for detector; T.O. - Tektronix 7904 Oscilloscope.

could not be used as many pulses are required to obtain a trace. Hence a real-time oscilloscope, Tektronix model 7904 with 500-MHz bandwidth (risetime = 0.7 nsec) was used. The photodetector used to detect the pulses was Tropel 330, having a risetime of 0.3 nsec. Since the laser produced<sup>13</sup> 25-psec pulses, the response of the detection system was -0.8 nsec, as verified using 30 cm of fibre. This is shown in figure 2 with the pulse separation being 8 nsec. A dispersion of -1 nsec has to occur in the fibre so that, when convolved with the system response time, a change of one small division, corresponding to 0.4 nsec, can be observed in the output pulses on the oscilloscope.

Using a He-Ne laser, the system was aligned with the test fi-

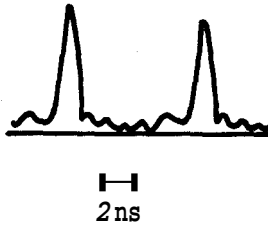


Fig.2 - Response of the detection system to the 25-psec mode-locked ruby pulses measured with 30 cm of fibre. Pulse separation is 8 nsec.

bre placed in the fibre-mounts so that accumulation of dust particles on the ends was avoided. Microscope objective  $M_1$  focused the light into the fibre and was changed, when needed, to alter the beam semi-angle, i. e., the numerical aperture of the light launched. Microscope objective  $M_2$  ( $\times 45$ ) collimated the output light from the fibre and  $M_3$  ( $\times 10$ ) focused it onto the photodetector. The ruby laser beam was aligned into the system with the help of apertures  $A_1$  and  $A_2$ , which were removed afterwards. For experiments at 694 nm, no filter  $F_1$ , Raman cell R, or filter  $F_2$  were used. Filter  $F_3$  was used to attenuate the peak pulse power so that non-linear effects, e.g. stimulated Raman scattering, in the fibre were avoided.  $F_4$  was a narrow-band pass filter at 694 nm.

For the second series of experiments at a different wavelength, the Raman cell R, containing cinnamaldehyde, was inserted. The Stokes wavelength obtained by stimulated Raman scattering was 782 nm, with the ruby laser as the pump beam. A cell length of 20 cm was used to give a reasonable conversion efficiency.  $F_1$  attenuated the ruby pump so that self-focussing in the Raman cell was avoided.  $F_2$  was a cut-off filter at 694 nm and  $F_4$  was narrow-band pass filter at 782 nm. The output wavelength from the Raman cell was confirmed by measuring the transmission through narrow-band filters and by passing the output light through a Hilger and Watts grating monochromator. For the third series of experiments at 871 nm, acetone was inserted into the Raman cell and  $F_4$  was changed to a narrow-band filter at this wavelength. Table 1 contains a summary of the Raman liquids used, their vibrational frequencies and the Stokes wavelengths obtained.

Table 1 - Raman liquids used and their characteristics.

Raman Liquid	Vibrational frequency $\Delta k$ ( $\text{cm}^{-1}$ )	$k_s$ ( $\text{cm}^{-1}$ )	$\lambda_s$ (nm)
Cinnamaldehyde	1655	12748	782.4
Acetone	2925	11478	871.2

$$\lambda_p = 694.3 \text{ nm} ; k_p = 14403 \text{ cm}^{-1}$$

Subscripts:  $p$  = pump ;  $s$  = Stokes

### 3. RESULTS OBTAINED

The results were obtained with two different types of multi-mode fibres<sup>16</sup>, both having step-index difference between core and cladding. One was a solid-core fibre (GCF) and the other two were liquid-core fibres (LCF). Their characteristics are out-lined in Table 2. The fibres were loosely wound on expanded polystyrene drums with a diameter of 45 cm. The fibre mounts, as shown in figure 1, were filled with index-matching liquid for the GCF and the core liquid with the LCF.

To determine the launching beam semi-angle ( $\theta$ ) in the core, it was necessary to measure the spatial distribution of the ruby laser, and the light beams at 782 and 871 nm, at the position of the launching objective  $M_1$ . This was done with a linear photodiode array and the result for the ruby beam ( $\lambda = 694 \text{ nm}$ ) is shown in figure 3. The spot-size, as determined from this figure was 0.9 mm. Using a  $\times 20$  microscope objective  $M_1$ , of focal length 8 mm,  $\theta = 4^\circ$  to the  $e^{-2}$  x maximum intensity points of the Gaussian distribution. As pointed out earlier, we needed  $\theta > 3^\circ$  to observe a distinct change in the output pulses, since the length of the GCF is comparatively short and the system response is  $\approx 0.8 \text{ nsec}$ . The input was heavily attenuated with filter  $F_3$  to ensure

Table 2 - Characteristics of the fibres tested

Nº	Fibre diameter ( $\mu\text{m}$ )	Core diameter ( $\mu\text{m}$ )	Cladding thickness ( $\mu\text{m}$ )	Fibre length (meters)	Core material	Cladding material
1 (GCF)	95	55			Schott F7 glass	ME1 Chance Pilkington tube
2 (LCF)	140	100	20	110	(Liquid) Hexachlorobuta 1,3-diene	ME1 Chance Pilkington tube
3 (LCF)	140	100	20	850	(Liquid) Hexachlorobuta 1,3-diene	ME1 Chance Pilkington tube

that no depletion of the probe pulse occurred due to nonlinear effects in the fibre. The output pulse shape was photographed after suitably pre-fogging the polaroid film and the full width at half-maximum (FWHM) intensity points was measured to be 1.6 nsec. After deconvolution of the system response, assuming Gaussian pulse shapes, we calculated a dispersion of 1.25 nsec in 55 m of fibre, i.e. 23 psec/m. This was entirely due to multi-path propagation, i.e. dispersion caused by the differences in the group velocities of the various propagating modes. Material dispersion, or chromatic dispersion, due to the wavelength dependence of the core refractive index and the spectral width (~200 GHz) of the probe pulse was negligible.

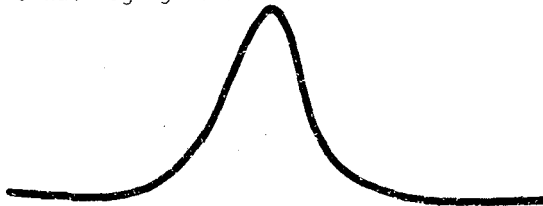


Fig.3 - Spatial Intensity distribution (Gaussian) of the ruby beam at the position of the coupling objective, 50 cm from the output mirror of the laser oscillator, measured with a linear photodiode array. Spot-size = 0.9 mm.

In order to verify mode conversion effects within the fibre, we measured the output semi-angle with the linear photodiode array. The result obtained is shown in figure 4 (a). The output semi-angle measured in air ( $\theta'$ ) is  $10^\circ$ , and hence  $\theta = 6^\circ$  in the fibre core. The launching was carried out at  $\alpha = 4^\circ$ ; hence the angular width had increased due to mode conversion, most probably due to the bend radius of the fibre of 22.5 cm. The results shown in figure 4 (b) and 4 (c) were obtained at 782 nm and 871 nm respectively and are discussed below.

For the measurements at 782 and 871 nm, the ruby pump power into the Raman cell was attenuated sufficiently to ensure that no self-focussing effects occurred in the cell. These effects can cause significant beam divergence and hence change the launching conditions, especially  $\theta$ , drastically. We again measured the spatial distribution of these Raman beams to verify a Gaussian distribution and its width for calculation of  $\theta$  accurately. The result, for the 871 nm beam, is shown in figure 5, indicating that the deviation from a Gaussian shape is not significant. We again launched with  $\theta = 4^\circ$  and the measured dispersion

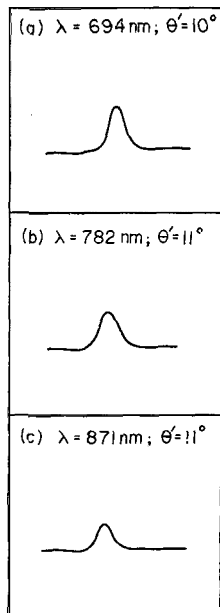


Fig.4 - Output angular distributions at three wavelengths after 55m of glass-core fibre (GCF).  $\theta'$  is the output semi-angle in air to the point where intensity falls to  $e^{-2}$  maximum intensity.

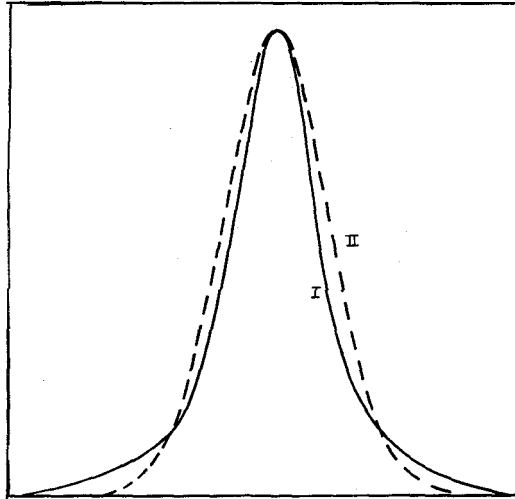


Fig.5 - Gaussian fitted to the spatial distribution of the Raman beam at 871 nm. I is the Raman beam; II is the Gaussian fitted to the peak intensity and where it falls to  $e^{-2}$  maximum intensity.

and pulse shape were identical, within the measurement error of 0.2nsec, to that at 694 nm. The output angles at 782 nm and 871 nm were measured, as before and are shown in fig. 4 (b) and 4 (c). We noted that these angles at the three wavelengths were within 10% of each other. We made further checks of these results by measuring pulse dispersion in the GCF at  $\theta = 0.3^\circ$ ,  $2^\circ$  and  $8.5^\circ$  for the three wavelengths. For the first two angles, no dispersion was resolved in each case due to system response, while for  $\theta = 8.5^\circ$ , the dispersion was  $\approx 35$  psec/m, being similar within measurement error for each wavelength.

The results with the liquid-core fibres follow the same trend as the above results with GCF and again emphasize the strong dependence of dispersion on  $\theta$ . We illustrate one result obtained in figure 6, which shows the output pulses at 694 nm and 871 nm, indicating a dispersion of 4.4 ns in 850 m of LCF, or 5.2 psec/m for  $\theta = 0.3^\circ$ . The pulse separation in the pulse train was  $\approx 8$  nsec, and hence a higher launching angle could not be used for this length as the larger pulse dispersion could not be unambiguously resolved. For the 110 m of LCF, with  $\theta = 0.3^\circ$  and  $2.5^\circ$ , the dispersion was  $< 8$  psec/m, not resolved due to system response. For  $\theta = 9^\circ$ , the dispersion was  $14 \pm 2$  psec/m at all three wavelengths.



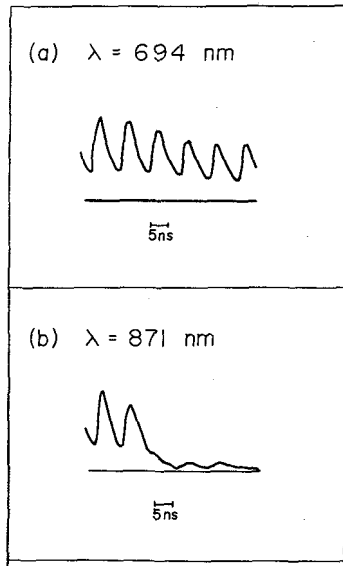


Fig.6 - Output pulses at two wavelengths after 850 m of liquid-core fibre (LCF) with the same launch semi-angle of  $0.3^\circ$  in the core. Pulse dispersion is 4.4 nsec or 5.2 psec/m.

#### 4. DISCUSSION

A change in the wavelength of the launched light can lead to a change in the refractive indices of the core and cladding and hence to a change in the numerical aperture of the fibre and in  $\theta$  in the core. Further, it can also lead to a change in the fibre attenuation, due to the attenuations of the core and cladding materials and the magnitude of Rayleigh scattering, which is inversely proportional to the fourth power of the wavelength. The core attenuation has the same effect on each propagating ray (or mode) and hence cannot lead to a wavelength dependence of dispersion. On the other hand, it has been shown by Gambling et al.<sup>17</sup> that a high loss of the cladding material can lead to a reduction in pulse dispersion by the mechanism of mode filtering of the higher order modes at a penalty of increased loss. This is because their fields penetrate further into the cladding compared to the lower order modes. Hence we can envisage a wavelength dependence of dispersion if there is a great amount of mode filtering at one wavelength compared to the others. Distinct observation of this effect would obviously depend on the number of modes filtered and the time resolution of the measurement system. Further, the number of modes excited in a particular fibre

is inversely proportional to the excitation wavelength. Therefore if there is no mode mixing or mode filtering in the fibre, a wavelength dependent dispersion is again possible but this is due to the launching, i.e. different number of modes excited, and not propagation effects in the fibre. We now discuss the results of our measurements with the above arguments in mind.

In the GCF, the refractive indices of both the core (F7) and cladding (ME1),  $n_1$  and  $n_2$ , decrease with increase in the wavelength ( $\lambda$ ); hence the numerical aperture (N.A.) of the fibre remains virtually unchanged at 0.64. The N.A. of the LCF is also unaltered from 0.43. Since the numerical aperture was not filled in both cases (i.e. not all modes excited), it is more important to determine how  $\theta$  in the core changed. For Schott F7 glass, the core in the GCF,  $n_1$  decreases from 1.618 to 1.611 (i.e. 0.43%) as  $\lambda$  increases from 694 to 871 nm. In hexachlorobuta 1,3-diene, the core in LCF,  $n_1$  decreases from 1.547 to 1.537 (0.68%) at the wavelengths mentioned. Hence, in both cases, there is a negligible change in  $\theta$  with the three wavelengths used in the experiments. Further, as the output angles are also very similar, though slightly increased compared to the input angles, it is not surprising to find that with the ray propagation model<sup>5</sup> in mind, the pulse dispersion is not dependent on the wavelength of the propagation rays. The output angles, as shown in fig. 4 show a 10% difference. If propagation was at these angles through the whole length of the fibre, the difference in the pulse dispersion, from the ray propagation model, would be 4 ps/m. This calculated difference was within experimental accuracy and hence was not resolved; the actual difference would be smaller as the beam width at launching was smaller compared to the beam widths measured at the output. These calculations and results demonstrate that launching conditions are very similar as the refractive index of the core alters very slightly.

Now we address ourselves to the effect of the cladding loss in our measurements. Gambling et al.<sup>17</sup> measured the bulk absorption loss ( $\alpha_k$ ) of the cladding material (ME1) in both GCF and LCF, in an unclad fibre form, at 694, 782 and 871 nm to be 1640, 1580 and 1520 db/km respectively, i.e. of the same order of magnitude. The loss coefficient ( $k$ ), given by them as

$$k = \frac{\lambda \alpha k}{4\pi}$$

undergoes a maximum change of only - 16% and this causes a negligible change in the pulse shapes, as predicted by their theory for a much longer length (180 m) and a larger  $\theta$  of  $8^\circ$ . Some change in the dispersion could be expected if the loss at one wavelength was at least an order of magnitude different from that at another wavelength. These calculations clearly show that, for these fibres, there is no preferential mode filtering as a function of wavelength and is confirmed by the experimental results of measuring the output angle. A significant mode filtering would be accompanied by a reduction in the output angle. Since the bulk attenuations of the core in the GCF and LCF are different by an order of magnitude, these measurements further demonstrate that pulse dispersion and shape are not dependent on the loss of the core material, as each ray, or mode, suffers the same attenuation.

Our measurements are in good agreement with those made by Gloge *et al.*<sup>9</sup> at 568 and 647 nm, with a mode-locked krypton-ion laser. No change in pulse shape or dispersion was observed for a particular  $\theta$  launching. When the focal length of the coupling lens was decreases, i.e.  $\theta$  increased, an increase in dispersion occurred, as previously predicted theoretically and observed experimentally<sup>5</sup>. Although it was stated that the results at 1.06  $\mu\text{m}$  were essentially the same, it is only apparent that launching was done at the same angle. Coupling with the same microscope objective does not necessarily mean an identical  $\theta$  as the beam widths ( $w$ ) could, be different from different lasers;  $w$  depends on the radii of curvature of the cavity mirrors, their separation, the oscillating wavelength and the distance of the coupling lens from the output mirror. We have extended these measurements to four different  $\theta$  at three wavelengths for two different fibre types. Further, by measuring the output angle we have shown that the mode conversion or filtering effects are not dependent on the wavelength.

Burrus *et al.*,<sup>8</sup> have also measured the impulse response in fibres having different refractive index profiles at 0.633, 0.9 and 1.06  $\mu\text{m}$ . Although the absolute values of dispersion were different for the different fibres, the results are quoted to be essentially similar at all three wavelengths.

Pulse dispersion, dominated by material dispersion, will have a very marked dependence on the wavelength of the light in optimum graded-index fibres excited by light emitting diodes. This will be discussed further in a separate publication<sup>18</sup>.

## 5. CONCLUSIONS

We have carried out measurements of pulse dispersion in two different types of multimode step-index fibres, at three wavelengths, namely 694, 782 and 871 nm, and observed negligible change provided the launching was carried out at the same beam semi-angle. The mode conversion was small but also similar as verified by measurements of the output angle at each wavelength. As the launching angle and the output angle were similar in each case, it was to be expected that the dispersion was also similar.

The measurements were carried out<sup>5</sup> at Southampton University and I thank Professor W.A. Gambling for the facilities provided; Dr. D. N. Payne for supplying the fibres and for many stimulating discussions. I am especially indebted to Professor G.D. Sims for his guidance and encouragement, at times most needed.

## REFERENCES

1. H.R.D. Sunak and J.B.M. Ayres Neto, "Medidas do coeficiente de conversão de modos em fibras Óticas multimodo", *Revista Brasileira de Física*, 9(1), 205-216 (1979).
2. H.R.D. Sunak and J.B.M. Ayres Neto, "Intermodal Pulse Dispersion in multimode Optical Fibres and its measurement with a Nanosecond Test Facility", *Revista Brasileira de Física*, this issue.
3. H.R.D. Sunak and J.B.M. Ayres Neto, "Intermodal Pulse Dispersion in multimode Optical Fibres and its measurement with a Nanosecond Test Facility", *Revista Brasileira de Física*, (this issue), 10(3), 000-000, September 1980.

3. J.B.M. Ayres Neto, "Efeitos de propagação em fibras óticas multimodo", Masters Thesis, Universidade Estadual de Campinas, Instituto de Física, Campinas, September 1979.
4. H.R.D. Sunak and J.B.M. Ayres Neto, "Material dispersion measurements in fibre optical waveguides", Revista Brasileira de Física (this issue), 10(3),000-000, September, 1980.
5. H.R.D. Sunak, "Experimental Study of pulse dispersion in multimode optical fibre waveguides", Ph. D. Thesis, University of Southampton, Southampton, U.K., 1975.
6. P.W. Smith, "Mode-locking of lasers", Proc. Inst. Elect. Electron. Eng., 58, 1342-1357 (1970).
7. H.R.D. Sunak, "Advances in fibre-optical communication systems", Electronics and Power, 19, 528-532, November 1973.
8. C.A. Burrus, E.L. Chinnock, D. Gloge, W.S. Holden, Tingye Li, R.D. Standley and D.B. Keck, "Pulse Dispersion and refractive-index profiles in some low-noise multimode optical fibres", Proc. Inst. Elect. Electron. Eng., 61, 1498-1499 (1973).
9. D. Gloge, E.L. Chinnock, R.D. Standley and W.S. Holden, "Dispersion in a low-loss multimode fibre measured at three wavelengths", Electronics Letters, 8, 527-529 (1972).
10. V.N. Smiley, H.F. Taylor, A.L. Lewis and D.J. Albares, "Pulse distortion in fibre optic bundles", Applied Optics, 10, 2543-2545 (1971).
11. D. Gloge, A.R. Tynes, M.A. Duguay and J.W. Hansen, "Picosecond pulse dispersion in optical fibres", IEEE Journal of Quantum Electronics, QE-8, 217-221 (1972).
12. H.R.D. Sunak and W.A. Gambling, "Picosecond pulse dispersion in cladded glass fibre", Optics Communications, 11(3), 277-281, July 1974.
13. M.W. McGeoch, "The production and measurement of ultrashort pulses in a ruby laser", Optics Communications, 7, 116-120 (1973).
14. E.L. Chinnock, L.G. Cohen, W.S. Holden, R.D. Standley and D.B. Keck, "The length dependence of pulse spreading in the CGW-Bell-10 optical fibre", Proc. Inst. Elect. Electron. Eng., 61, 1499-1500 (1973).
15. S.E. Miller, E.A.J. Marcatili and Tingye Li, "Research toward optical-fibre transmission systems, I and II", Proc. Inst. Elect. Electron. Eng. 61, 1703-1751 (1973).
16. D.N. Payne and W.A. Gambling, "The preparation of multimode glass-and liquid-core optical fibres", Opto-Electronics, 5, 297-307 (1973).

17. W.A. Gambling, D.N. Payne and H. Matsumura, "Effect of loss on propagation in multimode fibres", *Radio and Electronic Engineer*, 43, 683-688 (1973).
18. H.R.D. Sunak, "Material dispersion in optical fibre waveguides and techniques for its measurement", to be published.